Pressure-Induced Valence Tautomerism in Cobalt *o*-Quinone Complexes: An X-ray Absorption Study of the Low-Spin [Co^{III}(3,5-DTBSQ)(3,5-DTBCat)(phen)] to High-Spin [Co^{II}(3,5-DTBSQ)$_2$(phen)] Interconversion

Cecile Roux,[1a,d] David M. Adams,[1b] Jean P. Itié,[1c] Alain Polian,[1c] David N. Hendrickson,*[,1b] and Michel Verdaguer*[,1a]

Laboratoire de Chimie des Métaux de Transition (URA, CNRS 419) and Laboratoire de Physique des Milieux Très Condensés (URA, NCRS 782), Université P et M. Curie, 4 Place Jussieu, 75252 Paris, Cedex 05, France, and Department of Chemistry-0358, University of California at San Diego, La Jolla, California 92093-0358

Received August 18, 1995[⊗]

The temperature- and pressure-driven solid state valence tautomeric transformations of [Co^{II}(3,5DTBSQ)$_2$(phen)]·C_6H_5-CH) and nonsolvated [Co^{II}(3,5DTBSQ)$_2$(phen)] have been studied by EXAFS and XANES. When the toluene solvate sample is cooled it converts in the 270−215 K region (T_c = 240 K) from a high-spin Co^{II} complex at higher-temperatues to a low-spin Co^{III} complex at temperatures below ∼215 K. EXAFS data indicate that the HS-Co^{II} tautomer has bond lengths of Co−O = 2.08 ± 0.02 Å and Co−N = 2.13 ± 0.02 Å, whereas the LS-Co^{III} tautomeric complex is smaller with Co−O = 1.91 ± 0.02 Å and Co−N = 1.93 ± 0.02 Å. The XANES spectra obtained in the 270−215 K interconversion region were simulated to obtain a plot of the fraction of HS-Co^{II} complexes, n(HS-Co^{II}), vs temperature. This plot of n vs T agrees with that obtained from magnetic susceptibility data for the toluene solvate. In the XANES spectral region transitions characteristic of either a HS-Co^{II} or a LS-Co^{III} complex could also be used to monitor the valence tautomeric conversion. The nonsolvated phen complex does not convert at low temperatures (2 K) to a LS-Co^{III} tautomer. However, both complexes could be driven from the larger HS-Co^{II} form to the smaller LS-Co^{III} form upon application of pressure. EXAFS and XANES data readily detected these changes. For the toluene solvate, this conversion occurred within the 0.075−0.700 GPa range with a midpoint of $P_c\uparrow$ = 0.370 GPa. The nonsolvated complex required higher pressures of 0.10−2.5 GPa with $P_c\uparrow$ = 1.1 GPa. These are the first reported examples of valence tautomeric transformations driven by pressure. Both the thermally driven and pressure-driven valence tautomeric transformations are found to be reversible.

Introduction

Cobalt complexes with two *o*-quinone derived ligands have been shown to undergo a thermally driven valence tautomeric interconversion.[2−4] Recently, we have shown that the same valence tautomerism can also be photoinduced in solution as well as in polymer films.[5] The large changes in optical and magnetic properties which accompany this interconversion make these complexes candidates for molecular switching devices.[6] The valence tautomeric interconversion is depicted in eq 1,

$$\text{low-spin } [Co^{III}(SQ)(CAT)(N\frown N)] \overset{T,\,h\nu,\,P}{\rightleftharpoons} \text{high-spin } [Co^{II}(SQ)_2(N\frown N)] \quad (1)$$

where N⌒N refers to a chelating diiminium ligand such as 2,2′-bipyridine and SQ^- and CAT^{2-} refer, respectively, to the singly and doubly reduced forms of an *o*-quinone ligand. The two tautomers are related both by intramolecular electron transfer between a catecholate ligand and the cobalt ion and a spin change at the cobalt center. Since this conversion from *high-spin* Co^{II} (HS-Co^{II}) to *low-spin* Co^{III} (LS-Co^{III}) tautomers is accompanied by a shortening of the metal−ligand bond lengths and hence the molecular and crystal unit-cell volumes, pressure may also act as an external perturbation. The system is thermodynamically governed by the relationship $(\delta G/\delta P)_T = V$. Thus, at a certain critical pressure the LS-Co^{III} tautomer may become thermodynamically stabilized relative to the HS-Co^{II} form. Although pressure induced spin-crossover has been studied in Co^{II} [7−9]and Fe^{II} [10−22]complexes, no such study has been performed on a complex involving intramolecular electron transfer.

In this paper we present the first pressure induced valence tautomeric *high-spin* $Co^{II}(SQ)_2$ to *low-spin* $Co^{III}(SQ)(CAT)$ interconversion and show that X-ray absorption spectroscopy is a good technique to follow such a transformation. The compounds studied are the toluene-solvated complex [Co^{II}-(3,5DTBSQ)$_2$(phen)]·$C_6H_5CH_3$ (complex **A**) and the nonsolvated complex [Co^{II}(3,5DTBSQ)$_2$(phen)] (complex **B**). 3,5-DTBSQ$^-$ and 3,5-DTBCAT^{2-} refer, respectively, to the singly and doubly reduced forms of 3,5-di-*tert*-butyl-*o*-quinone and phen refers to 1,10-phenanthroline. Complex A is the only compound known to exhibit an abrupt thermally driven valence tautomeric interconversion in the solid-state.[2] On the other hand the nonsolvated complex **B** was shown to persist as a high-

⊗ Abstract published in *Advance ACS Abstracts,* April 15, 1996.

(1) (a) Laboratoire de Chimie des Métaux de Transition, Université P et M. Curie. (b) Department of Chemistry-0358, University of California at San Diego, La Jolla, California 92093−0358. (c) Laboratoire de Physique des Milieux Très Condensés, Université P et M. Curie. (d) Present address: Laboratoire de Chimie de la Matiere Condensee, Universite P. et M. Curie, 4 Place Jussieu, 75252 Paris Cedex 05, France.

(2) (a) Adams, D. M.; Dei, A.; Rheingold, A. L.; Hendrickson, D. N. *Angew. Chem.* **1993**, *105*, 954. (b) Adams, D. M.; Dei, A.; Rheingold, A. L.; Hendrickson, D. N. *J. Am. Chem. Soc.* **1993**, *115*, 8221.

(3) Abakumov, G. A.; Cherkasov, V. K.; Bubnov, M. P.; Ellert, O. G.; Dobrokhotova, Z. B.; Zakaharov, L. N.; Struchov, Y. T. *Dokl. Akad. Nauk.* **1993**, *328*, 12.

(4) (a) Jung, O. S.; Pierpont, C. G. *Inorg. Chem.* **1994**, *33*, 2227. (b) Jung, O. S.; Pierpont, C. G. *J. Am. Chem. Soc.* **1994**, *116*, 1127. (c) Pierpont, C. G.; Lange, C. W. *Prog. Inorg. Chem.* **1994**, *41*, 331.

S0020-1669(95)01080-9 CCC: $12.00

spin Co^{II} tautomer down to 2 K.[2] In this study the thermal and pressure induced valence tautomeric interconversion is monitored by observing changes in the structures of the X-ray absorption spectrum.

Experimental Section

Syntheses. The compounds were prepared as previously described.[2] All samples gave good elemental analyses.

High-Pressure Cell. A Block-and-Piermarini diamond-anvil cell[23] was used to generate the high pressures. Silicone oil was used as the pressure transmitting medium. To measure the pressure a small ruby chip was added to the samples. Pressure measurements were performed by following the shift of the R_1 transition (at 694.2 nm under atmospheric pressure) excited by the 488 nm line of an air-cooled argon laser following the relation $P = \Delta\lambda/3.65$ GPa. Further details of the experimental setup and conditions have been presented elsewhere.[7]

Recording of XANES Spectra. X-ray absorption experiments were carried out on two dispersive mode EXAFS stations at LURE (Paris-Sud University). Variable temperature spectra were recorded at the conventional EXAFS III station which is equipped with a Si 311 double crystals monochromator and ionization gas chambers and used in the step by step mode.[24] The EXAFS spectra were recorded with 2 eV steps in a 1000 eV energy range. The XANES spectra were recorded with 0.25 eV steps in a 150 eV energy range. The deep hole energy width at this energy is ≈1 eV, and the experimental resolution is also ≈1 eV. The XANES recording mode ensures a reproducibility better than 0.25 eV. The variable pressure spectra were recorded at the dispersive mode EXAFS station.[25] The detector position was optimized at the monochromatic focus point to achieve a resolution ≈1 eV. The DCI storage ring was operated at 1.85 GeV with a typical current of 300 mA. For the variable pressure measurements, owing to the strong absorption of diamonds and to the limited thickness of the samples, the data collection time was 6 s. In order to increase the statistics, 32 spectra were added for each pressure. Further details of the experimental setup have been described previously.[7]

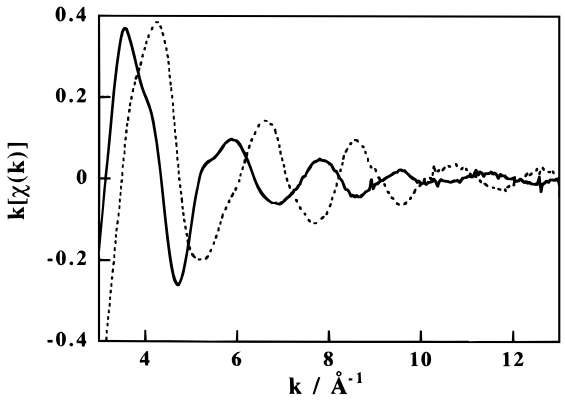

Figure 1. Co K-edge EXAFS spectra k[χ(k)] for complex **A** at $T = T_{amb}$ (- - -) and T = 200 K (—).

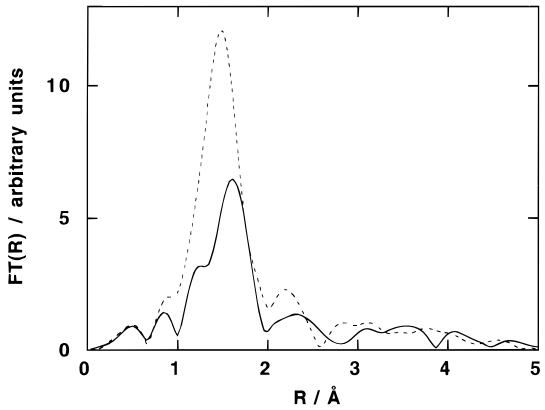

Figure 2. Modulus of the Fourier Transform in the R space at $T = T_{amb}$ (- - -) and T = 200 K (—) for complex **A**.

Results

For complex **A**, the Co K-edge EXAFS spectra, $k[\chi(k)]$ vs k, obtained in variable temperature experiments under atmospheric pressure (P_{atm}) from ambient temperature (T_{amb}) to $T = 200$ K are shown in Figure 1. Figure 2 gives the modulus part of the corresponding Fourier transforms as $\rho(R) = \int k^3\chi(k)\omega(k)\,dk$ where $\omega(k)$ is the Kaiser window function used (τ is 2.5), in the R space at $T = T_{amb}$ and $T = 200$ K. The 200K FT spectra show an envelope similar to the one at $T = T_{amb}$, *i.e.*, only a single peak; however, the oscillations are displaced to lower distances, and the Debye-Waller factor (σ) has decreased.

The EXAFS data obtained at $T = T_{amb}$ and $T = 200$ K have been fit. At each temperature the parameters are the Debye−Waller factor (σ), the ionization energy (E^0), the metal−ligand distance (R), and the parameter Γ used to define the mean free path of the electron $\lambda(k)$ by the formula $\lambda(k) = (k/\Gamma) + (\eta/k)^4$, with $\eta = 3.1$. In order to avoid fits without physical meaning, we have constrained the number of fitted parameters to the minimum. In particular, we have chosen the same values of Γ and E^0 for the two subshells of the first shell of neighbors for each complex and the experimental results were fit using Teo and Lee parameters,[25c] with a distribution of neighbors equal to 4O and 2N and with R values close to the crystallographic ones.[2] The quantitative analysis of the EXAFS data for the first shell is summarized in Table 1. This table also gives some structural and magnetic data which are described below. The second shell of neighbors includes essentially the carbon skeleton of the ligands which is more or less separated from the first shell. We did not attempt to analyze the second shell.

(5) Adams, D. M.; Li, B.; Simon, J. D.; Hendrickson, D. N. *Angew. Chem.* **1995**, *34*, 1481.
(6) (a) Hauser, A. *Chem. Phys. Lett.* **1993**, *202*, 173. (b) Kahn, O.; Kröber, J.; Jay, C. *Adv. Mater.* **1992**, *4*, 778. (c) Hush, N. S.; Wong, A. T.; Balskay, G. B.; Reimers, J. R. *J. Am. Chem. Soc.* **1990**, *112*, 4192.
(7) Roux, C.; Zarembowitch, J.; Itie, J. P.; Verdaguer, M.; Dartyge, E.; Fontaine, A.; Tolentino, H. *Inorg. Chem.* **1991**, *30*, 3174.
(8) Salloni, L.; Ferraro, J. R. *Inorg. Chim. Acta*, **1974**, *9*, 49.
(9) Stephens, D. R.; Drickamer, H. G. *J. Chem. Phys.* **1961**, *35*, 429.
(10) Fisher, D. C.; Drickamer, H. G. *J. Chem. Phys.* **1971**, *54*, 4825.
(11) Bargeron, C. B.; Drickamer, H. G. *J. Chem. Phys.* **1971**, *55*, 3471.
(12) Ferraro, J. R.; Takemoto, J. *Appl. Spectrosc.* **1974**, *28*, 66.
(13) Butcher, R. J.; Ferraro, J. R.; Sinn, E. *Inorg. Chem.* **1976**, *15*, 2077.
(14) Haller, K. J.; Johnson, P. L.; Feltham, R. D.; Enemark, J. H.; Ferraro, J. R.; Basile, L. J. *Inorg. Chim. Acta* **1979**, *33*, 119.
(15) Long, G. J.; Becker, L. W.; Hutchinson, B. B. *Adv. Chem. Ser.* **1981**, *194*, 453.
(16) Adams, D. M.; Long, G. J.; Williams, A. D. *Inorg. Chem.* **1982**, *21*, 1049.
(17) Pebler, J. *Inorg. Chem.* **1983**, *22*, 4125.
(18) Usha, S.; Srinivasan, R.; Rao, C. N. R. *Chem. Phys.* **1985**, *100*, 447.
(19) Long, G. J.; Hutchinson, B. B. *Inorg. Chem.* **1987**, *26*, 608.
(20) McCusker, J. K.; Zvagulis, M.; Drickamer, H. G.; Hendrickson, D. N. *Inorg. Chem.* **1989**, *28*, 1380.
(21) Köhler, C. P.; Jakobi, R.; Meissner, E.; Wiehl, L.; Spiering, H.; Gütlich, P. *J. Phys. Chem. Solids* **1990**, *51*, 239.
(22) (a) König, E.; Ritter, G.; Kulshreshtha, S. K.; Waigel, J.; Goodwin, H. A. *Inorg. Chem.* **1984**, *23*, 1896. (b) König, E.; Ritter, G.; Waigel, J.; Goodwin, H. A. *J. Chem. Phys.* **1985**, *83*, 3055.
(23) Le Toullec, J. P.; Pinceaux, J. P.; Loubeyre, P. *High Pressure Res.* **1980**, *1*, 77.
(24) (a) Dubuisson, J. M.; Dauvergne, J. M.; Depautex, C.; Vachette, P.; Williams, C. *Nucl. Instrum. Methods* **1986**, *A246*, 636. (b) Goulon, J.; Lemonnier, M.; Cortes, R.; Retournard, A.; Raoux, D. *Nucl. Instrum. Methods* **1983**, *208*, 6325. (c) Prieto, C.; Briois, V.; Parent, P.; Villain, F.; Lagarde, P.; Dexpert, H.; Fourman, B.; Michalowicz, A.; Verdaguer, M. *Synchrotron Radiation and Dynamic Phenomena, Grenoble 1991*; Conference Proceedings N 258; American Institute of Physics: New York, 1992; p 621.
(25) (a) Tolentino, H.; Dartyge, E.; Fontaine, A.; Tourillon, G. J. *J. Appl. Crystallogr.* **1988**, *21*, 15. (b) Tolentino, H.; Baudelet, F.; Dartyge, E.; Fontaine, A.; Lena, A.; Tourillon, G. J. *Nucl. Instrum. Methods Phys. Res.* **1990**, *A289*, 307. (c) Teo, B.-K.; Lee, P. A., *J. Am. Chem. Soc.* **1979**, *101*, 2815.

Table 1. Best Fit Parameters for the First Shell of Co^{II} Neighbors in $[Co^{II}(3,5DTBSQ)_2(phen)]\cdot(C_6H_5CH_3)$ (Complex **A**)

parameters[a]	$T = T_{amb}$	$T = 200$ K
First Subshell		
R_1, Å	2.13 (2.14[b])	1.93 (1.93[b])
σ_1, Å	0.12	0.08
no. and postulated nature of neighbors	2 N	2 N
Second Subshell		
R_2, Å	2.08 (2.05[b])	1.91 (1.89[b])
σ_2, Å	0.09	0.06
no. and postulated nature of neighbors	40	40
$E°$, eV	7708.5	7708.0
Γ	0.912	1.14
ρ	7×10^{-5}	7×10^{-4}
μ_{eff}, μ_B[c]	5.13	1.72

[a] The fitting parameters are as follows: Co−nitrogen distances (R_1); Co−oxygen (R_2) distances; Debye−Waller factor, σ_i; ionization energy, $E°$; and the constant Γ used to define the free mean path of the electron, $\lambda = k/\Gamma$. The agreement factor ρ is $\Sigma[\chi_{exp}(k) - \chi_{cal}(k)]^2$. [b] These bond lengths were determined with X-ray diffraction data. [c] Effective magnetic moment determined by magnetic susceptibility measurements.

No significant signal is present at a distance larger than 3 Å; in particular, no heavy atom contributions are observed, in agreement with the crystallographic data.[2]

That oxygen has a greater affinity than nitrogen for the Co^{II} ion is evidenced in the distances given by the X-ray diffraction data.[2] The EXAFS analysis leads to the same conclusion since the HS-Co^{II} tautomer observed at ambient temperature and $P = P_{atm}$ was found to have two different metal−ligand bond distances, 2.08 ± 0.02 and 2.13 ± 0.02 Å, attributed to four Co−O bonds and two Co−N bonds, respectively. At 200 K there is a complete conversion to the LS-Co^{III} tautomer as evidenced by magnetic susceptibility measurements.[2] At this temperature two different distances that are shorter than the previous ones were detected, 1.91 ± 0.02 Å (Co−O bonds) and 1.93 ± 0.02 Å (Co−N bonds).

A selection of the variable-temperature XANES spectra for complex **A** at $P = P_{atm}$ is given in Figure 3. Figure 4 presents selected XANES spectra of complex **A** obtained in a variable pressure experiment at $T = T_{amb}$. The pure HS-Co^{II} and LS-Co^{III} spectra determined with $P = P_{atm}$ at either $T = T_{amb}$ or $T = 200$ K, respectively, (see Figure 3) show a close similarity to the corresponding spectra obtained at $P = P_{atm}$ and $P = 1.5$ GPa (see Figure 4). Thus, the high-pressure cell does not affect the absorption curve and the LS-Co^{III} form induced either by low temperature or by a high pressure have similar molecular structures.

In the XANES range for complex **A** the main features characteristic of the HS-Co^{II} spectra are a strong slightly asymmetrical absorption at 7724.9 eV and two weak poorly resolved bands at 7708.2 and 7709.5 eV. The main spectral characteristics of the LS-Co^{III} form are a strong absorption at 7729.4 eV and a single weak well-defined absorption at 7709.9 eV. These transition energies are quite characteristic for octahedral HS-Co^{II} and LS-Co^{III} complexes. Other octahedral Co^{II} and Co^{III} complexes show similar transition energies.[26]

Finally, selected spectra recorded at different pressures for complex **B** with $T = T_{amb}$ are shown in Figure 5. It should be noted that the spectra of this compound at $P = P_{atm}$ and $P = 2.6$ GPa with $T = T_{amb}$ have the same general shape as the spectra for the pure HS-Co^{II} and LS-Co^{III} forms of complex **A**. At $P = 2.6$ GPa the conversion appears complete.

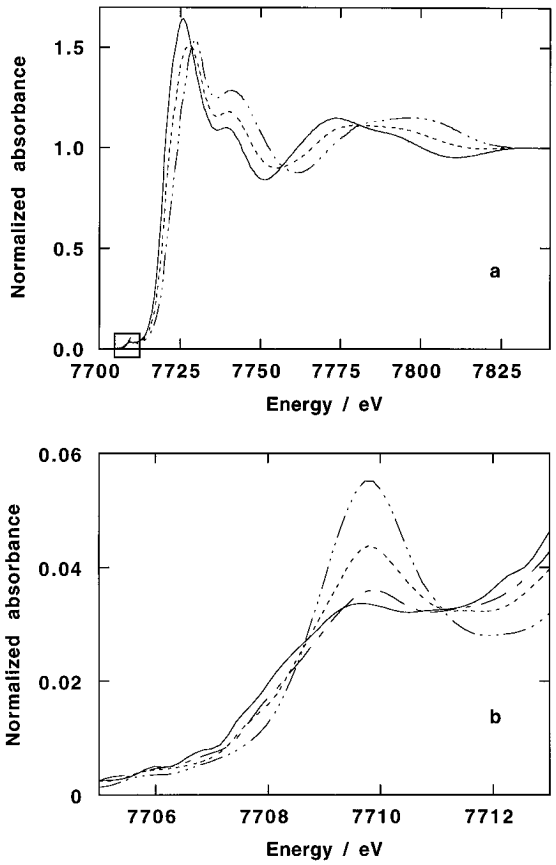

Figure 3. Near edge spectra of complex **A** at $T = T_{amb}$ (—), T = 252 K (— - —). T = 242 K (- - -) and T = 200 K (— - - - —) (a) in the full energy range and (b) in the preedge range. For clarity, the spectrum at $T = 252$ K in the all XANES range is omitted.

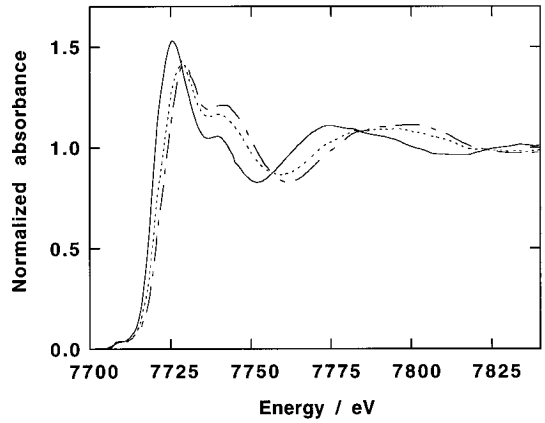

Figure 4. Selected near edge spectra obtained for complex **A** at room temperature under pressures of $P = P_{atm}$ (—), $P = 0.37$ GPa (- - -), and $P = 1.5$ GPa (— - —).

With the spectra for the pure HS-Co^{II} and LS-Co^{III} tautomers, it is possible to extract the values of the HS-Co^{II} fraction, n(HS-Co^{II}), at each temperature or pressure by comparing the experimental spectra with those calculated as a linear combination of the spectra of the HS-Co^{II} and LS-Co^{III} forms.[7] The good agreement obtained between experimental and simulated spectra is illustrated in Figure 6. Figure 7 shows the plot of n(HS-Co^{II}) as a function of temperature. The variable pressure experiments for both complexes A and B were performed first at increasing ($P\uparrow$) and then decreasing pressures ($P\downarrow$). The change of n(HS-Co^{II}) as a function of increasing and decreasing pressures is presented in Figure 8 for both compounds. The characteristic temperature and pressure values related to both compounds are collected in Table 2, where $T_{onset}\downarrow$ and $T_{end}\downarrow$ are

(26) Briois, V.; Cartier, C.; Momenteau, M.; Maillaro, P.; Zarembowitch, J.; Fontaine, A.; Tourillon, G.; Thuery, P.; Verdaguer, M. *J. Chim. Phys.* **1989**, *86*, 1623.

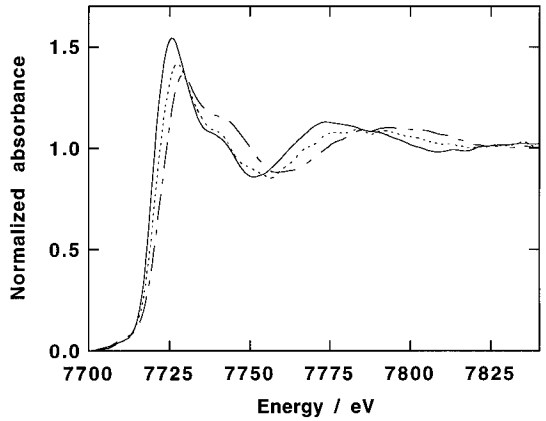

Figure 5. Selected near edge spectra obtained for complex **B** at room temperature under pressures of $P = P_{atm}$ (—), $P = 1.00$ GPa (- - -), and P = 2.0 GPa (- - -).

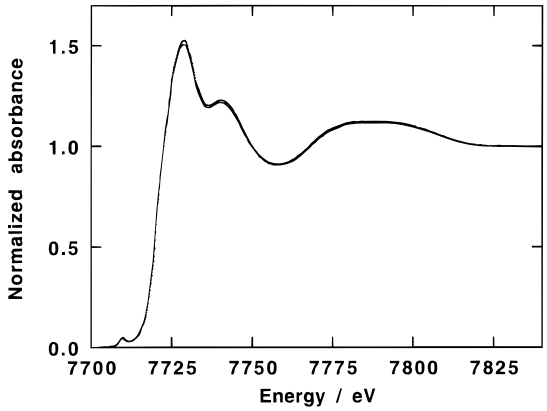

Figure 6. Comparison of the experimental spectrum for complex **A** at $T = 238$ K (•••) with the spectrum simulated for n(HS-Co^{II}) = 0.35 (—).

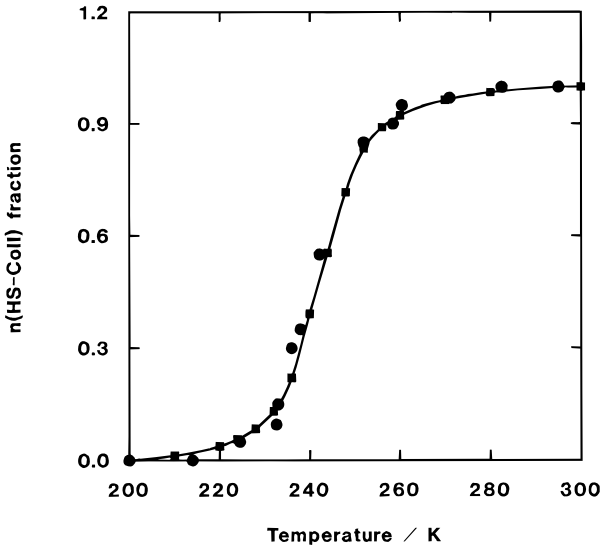

Figure 7. Plots of the HS-Co^{II} fraction n(HS-Co^{II}) as a function of temperature for complex **A**, determined by decreasing the temperature of a sample maintained at atmospheric pressure.

the temperature that correspond to the onset of and the end of the HS-Co^{II} to LS-Co^{III} conversion during the first decrease of the temperature, $P_{onset}\uparrow$ and $P_{end}\uparrow$ upon the first application of pressure, and $T_c\downarrow$ and $P_c\uparrow$ stand for the temperature and the pressure when n(HS-Co^{II}) = n(LS-Co^{III}) = 0.5. Table 2 also gives $T_{onset}\downarrow$, $T_{end}\downarrow$, and $T_c\downarrow$ for complex **A** as determined[2] by magnetic susceptibility data.

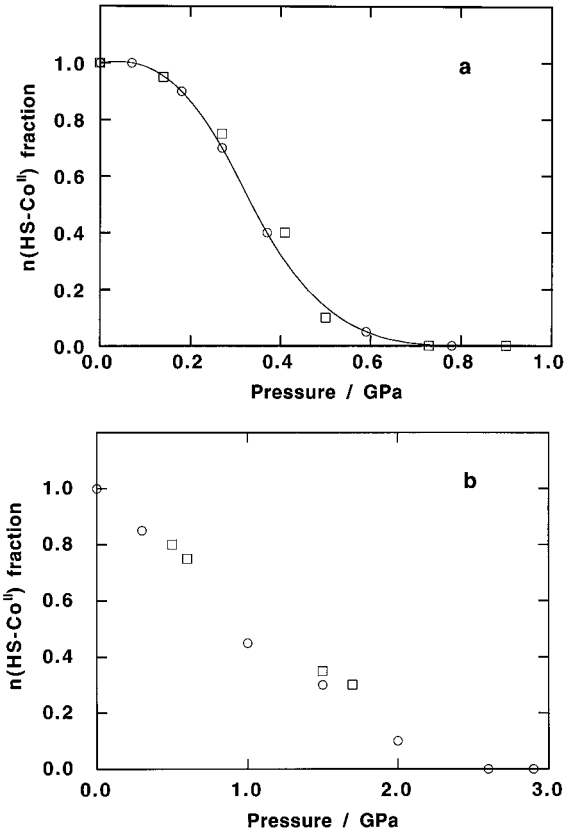

Figure 8. Plots of the HS-Co^{II} fraction n(HS-Co^{II}) as a function of pressure for complex **A** (a) and complex **B** (b) at room temperature and increasing (○) and decreasing (□) pressure.

Table 2. Characteristic Temperatures and Pressures[a] for the Valence-Tautomeric Transitions in [Co^{II}(3,5DTBSQ)$_2$(phen)]·$C_6H_5CH_3$ (Complex **A**) and [Co^{II}(3,5DTBSQ)$_2$(phen)] (Complex **B**)

	compound **A**	compound **B**
$T_{onset}\downarrow$, K	270 (260)[b]	c
$T_{end}\downarrow$, K	215 (220)[b]	c
$T_c\downarrow$, K	240 (238[a])	c
$P_{onset}\uparrow$, GPa	0.075	0.1
$P_{end}\uparrow$, GPa	0.700	2.5
$P_c\uparrow$, GPa	0.370	1.1

[a] See the text for a definition of the different temperatures and pressures. [b] Values determined by magnetic susceptibility measurements. [c] Complex **B** does not exhibit a thermally-induced valence-tautomeric transition.

Discussion

The above results clearly indicate that X-ray absorption spectroscopy is a sensitive technique to follow temperature or pressure induced valence tautomeric interconversions. This discussion concerns the interpretation of the edge structure as well as an analysis of the temperature and pressure changes on the X-ray absorption results.

(a) Interpretation of Edge Structures. In the XANES range, a one-electron description of the edge based on electric dipolar transitions only is unable to interpret all the features of the spectrum due to multielectron phenomena; however simple symmetry rules allow one to understand the main characteristic transitions.[27] The K-edge structures originate from transitions of the 1s core level of the metal to excited vacant states of proper symmetry involving metal orbitals. It is useful to a first approximation to consider the transitions as quasi-atomic. In atomic spectroscopy, with a electric dipolar operator,

(27) Cartier, P.; Verdaguer, M. *J. Chim. Phys.* **1989**, *86*, 1607.

Chart 1. Simplified Electronic Structures of the HS-Co^{II} and LS-Co^{III} Forms of Compounds **A** and **B**[a]

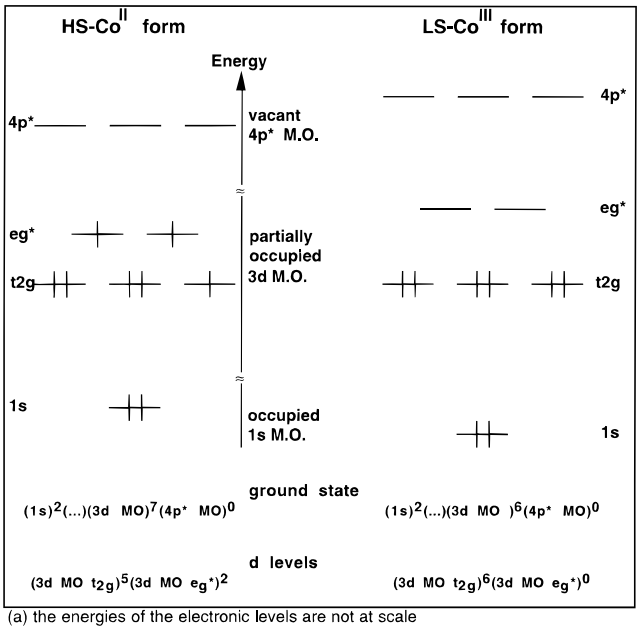

(a) the energies of the electronic levels are not at scale

the selection rule with respect to angular momentum is $\Delta l = \pm 1$. Thus, the XANES spectrum can be assigned as having the following components: (1) The preedge features are assigned to transitions of the 1s electron ($l = 0$) to metal d-levels ($l = 2$). These are formally dipolar forbidden ($\Delta l = 2$) and quadrupolar allowed and are usually weak in intensity with respect to the edge. (2) The edge structures are assigned to allowed transitions involving the 1s core levels ($l = 0$) to vacant metal p-orbitals ($l = 1$). In the case of molecular complexes, the symmetry can be lowered by the presence of ligands and p and d levels can mix (in T_d symmetry, for example). In the present case the cobalt center is close to O_h symmetry and the above rules apply fairly well. (3) Finally, the higher energy XANES features are assigned to multiple scattering and/or multi-electronic excitations which merge into the EXAFS range.

The simplified electronic structures of the HS-Co^{II} and LS-Co^{III} forms of the complex are schematized in Chart 1. The quasi-octahedral geometry of the coordination implies the degeneracy of the 4p* and e_g* antibonding levels. Upon passing from the HS-Co^{II} to LS-Co^{III} form, the $3d_{z^2}$ and the $3d_{x^2-y^2}$ orbitals become vacant. The bond length shortening associated with the valence tautomeric interconversion reflects changes in all the metal−ligand bonds. The geometry of the coordination core remains quasi-octahedral and the 4p* and 3d levels are expected to be destabilized without splitting. On the other hand, during the HS-Co^{II} to LS-Co^{III} conversion, the metal oxidation state increases, and this leads to a decrease in the screening effect, stabilizing the occupied orbitals, in particular the 1s orbital. The same reasoning leads to the conclusion that the weight of the metal 4p atomic orbitals in the vacant antibonding molecular orbital decreases with the HS-Co^{II} to LS-Co^{III} conversion, because of a larger participation of ligand orbitals due to shorter distances.

The room temperature XANES spectrum, Figure 3, of the HS-Co^{II} form of complex **A** is characteristic of weakly distorted octahedral *high-spin* Co^{II} complexes.[26] In the preedge area, two low-intensity features are seen at 7708.2 and 7709.5 eV that correspond, respectively, to the following dipolar-forbidden and quadrupolar-allowed transitions (O_h symmetry):

$$(1s)^2(...)(3d\ MO\ t_{2g})^5(3d\ MO\ e_g^*)^2 \rightarrow (1s')1(...')(3d\ MO'\ t_{2g})^6(3d\ MO'\ e_g^*)^2$$

$$(1s)^2(...)(3d\ MO\ t_{2g})^5(3d\ MO\ e_g^*)^2 \rightarrow (1s')1(...')(3d\ MO'\ t_{2g})^5(3d\ MO'\ e_g^*)^3$$

The prime sign means that the excited state of the molecular levels are relaxed in the core hole. In the edge area, the strong white-line band at 7724.9 eV is assigned to the symmetry-allowed transition

$$(1s)^2(...)(3d\ MO)^7(4p\ MO)^0 \rightarrow (1s')^1(...')(3d\ MO')^7(4p\ MO')^1$$

At higher energies, the weak shoulder at ∼7730 eV may be associated with a multiple-scattering process, whereas the features at 7750 eV are clearly single scattering EXAFS structures.

A similar interpretation of the 200K XANES spectrum of the LS-Co^{III} tautomeric state of complex **A** is possible (see Figure 3). In the preedge region, a single absorption at 7709.9 eV is observed with a higher intensity and may be assigned to the following dipolar-forbidden and quadrupolar-allowed transition:

$$(1s)^2(...)(3d\ MO\ t_{2g})^6(3d\ MO\ e_g^*)^0 \rightarrow (1s')^1(...')(3d\ MO'\ t_{2g})^6(3d\ MO'\ e_g^*)^1$$

For metallic complexes the Fermi golden rule implies that the density of vacant states N(E) plays an important part in the intensity of the preedge even in the case where the transition is dipolar forbidden.[27] In the LS-Co^{III} complex, the 1s → MO′ t_{2g} transition is no longer observed since the t_{2g} levels are fully occupied. On the other hand, the intensity of the 1s → MO′ e_g* transition is higher in the LS-Co^{III} form than in the HS-Co^{II} form because the e_g* levels are empty in the LS-Co^{III} form and singly occupied in the HS-Co^{II} form. In the edge area the intense absorption at 7729.4 eV is assigned to the following transition:

$$(1s)^2(...)(3d\ MO\ t_{2g})^6(4p\ MO)^0 \rightarrow (1s')^1(...')(3d\ MO't_{2g})^6(4p\ MO')^1$$

With respect to the HS-Co^{II} form, this transition is shifted by 4.5 eV to higher energies. This is caused by the shortening of the metal−ligand distances and by the increase in oxidation state. This important shift can be attributed to a simultaneous conversion of the spin and oxidation state, In fact, we observed only a shift of 2 eV in the case of an Fe^{II} octahedral complex exhibiting a thermally-induced spin transition in which the shortening of the mean metal−ligand distances is of the same order of magnitude, i.e. 0.16−0.24 Å. Furthermore, the decrease in white-line intensity in the LS-Co^{III} form may be accounted for by the shorter metal−ligand distances which enhance the mixture of ligand orbitals in the MO′ 4p*, reduce the participation of the metal orbitals in the wave function, and ultimately lead to a weaker intensity for the corresponding absorption. This band is much more symmetrical and intense ($I_{max} = 1.7$) than the band encountered in Co^{II} complexes exhibiting only a spin transition by temperature or pressure variation. In the case of octahedral compounds having the general formula [Co(H_2fsa$_2$-en)L_2], where H_2fsaen^{2-} is the phenolic dianion of the 2:1 condensation of 3-carboxysalicylaldehyde with 1,2-diaminoethane and L is an axial ligand such as water, pyridine, or 4-*tert*-

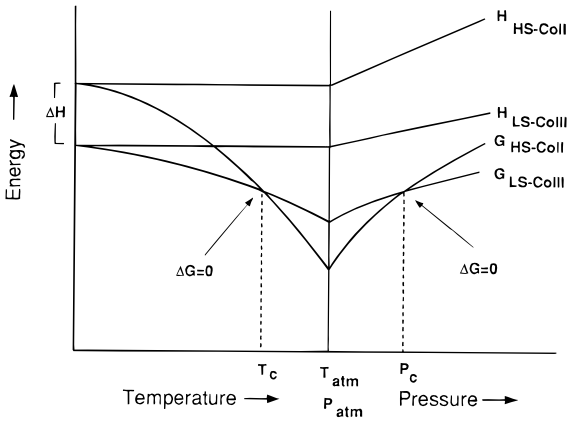

Figure 9. Qualitative thermodynamic diagram showing the variation of enthalpy *H* and Gibbs free energy *G* for the LS-Co^{III} and HS-Co^{II} tautomeric complexes as a function of temperature and pressure.

butylpyridine, two white-line absorptions are observed at 7734 eV ($I_{max} \sim 1.25$) and a weaker shoulder at 7724 eV in the LS-Co^{II} form.[7] This previous result was explained as attributable to the splitting of the 4p* levels due to the reduced equatorial metal−ligand bond distances. In the present case, the quasi-symmetrical absorption shows that all the metal ligand distances are similarly reduced during the conversion.

The interpretations of the data for the HS-Co^{II}(phen)(3,5-DTBSQ)$_2$ nonsolvated complex **B** are the same as those for the HS-Co^{II} form of complex **A**.

(b) Thermally Driven Valence Tautomeric Interconversions. In analogy to the extensively studied *high-spin* to *low-spin* spin-crossover phenomenon observed for iron and cobalt complexes, the interconversion between valence tautomers is an entropy driven process. At low temperatures the Co^{III} tautomer has an $S = {}^1/_2$ ground state (low-spin Co^{III} d^6 with one $S = {}^1/_2$ SQ$^-$ radical), whereas at higher temperatures the Co^{II} tautomer (high-spin Co^{II} $S = {}^3/_2$ with two $S = {}^1/_2$ SQ$^-$ radicals) has one $S = {}^5/_2$ state, one $S = {}^1/_2$ state, and two $S = {}^3/_2$ states thermally populated due to weak magnetic exchange interactions. There is an electronic entropy gain associated with the Co^{III}-to-Co^{II} conversion. As well, there is vibrational entropy gain due to the higher density of vibrational states in the HS-Co^{II} form. Thus, the thermal population of tautomeric states is dictated by the Gibbs free energy difference, $\Delta G = \Delta H - T\Delta S$. A qualitative thermodynamic diagram showing the variation of *G* and *H* with temperature is presented in Figure 9. In compounds that display a thermally driven valence tautomeric interconversion the Co^{II} tautomer zero-point energy must lie at higher enthalpic energy than that for the LS-Co^{III} form. At low temperatures $T\Delta S$ is negligible with respect to ΔH and consequently if $\Delta H > kT$ only the LS-Co^{III} state is populated. However, $T\Delta S$ is not negligible at higher temperatures. ΔG will change sign at a critical temperature T_c, where $\Delta G = 0$ and $\Delta H = T\Delta S$. At higher temperatures the HS-Co^{II} tautomeric state may be almost completely populated if ΔS is large enough.

As the temperature of the toluene solvated complex **A** is decreased from 298 to 270 K, there is little change in the XANES spectra. The complex retains the HS-Co^{II} form. Then, in the 270−215 K range, the complex converts from a HS-Co^{II} tautomer at 270 K to a LS-Co^{III} tautomer at 215 K. This transformation is reversible since the spectra at 298 K and at atmospheric pressure were found to be identical before and after the temperature treatment. The complete conversion occurs in a temperature range of ∼55 K, centered at $T_c = 240$ K. In Figure 7 is given a plot of the fraction of Co^{II} complexes, n(HS-Co^{II}), as a function of temperature. The data obtained from an analysis of the XANES spectra are plotted together with those evaluated from magnetic susceptibility data.[2] The two results are nearly identical and confirm that XANES data accurately track the valence tautomeric interconversion.

From the EXAFS data, the contraction ΔR of the mean coordination distance for the complete conversion from HS-Co^{II} to LS-Co^{III} is found to be 0.18 Å, which is close to the one determined[2b] in the single-crystal structural work, 0.205 Å. This value is larger than the ΔR contraction (0.09−0.12 Å) generally observed in cobalt(II) complexes exhibiting only a thermally-induced spin change without a change of oxidation state.[28,29] The order of magnitude is the same as the bond-length contraction seen for iron(II) spin-crossover complexes.[29]

(c) Pressure-Induced Valence Tautomeric Interconversions. The application of increasing pressure affects the enthalpic energy separation between valence tautomers according to the relationship

$$\Delta H = H_{\text{HS-Co}^{II}} - H_{\text{LS-Co}^{II}} = \Delta U + P\Delta V \qquad (2)$$

where ΔU is the internal energy change and ΔV is the volume change associated with the valence tautomeric conversion. Applying a pressure *P* results in an energy change $P\Delta V = P\Delta(V_{\text{HS-Co}^{II}} - V_{\text{LS-Co}^{III}})$, where ΔV is the volume difference of the crystal in the HS-Co^{II} and LS-Co^{III} tautomeric forms. The quantity $P\Delta V$ is positive since the HS-Co^{II} unit-cell volume is greater than the LS-Co^{III} unit-cell volume. Figure 9 displays a qualitative thermodynamic diagram showing the variation of *G* and H with pressure. Since ΔH becomes larger with increasing pressure, ΔG will change sign at a critical pressure P_c. At high enough pressure the Gibbs free energy of the LS-Co^{III} form is lower and its population increases with increasing pressure.

Complex **A** is known to exhibit a thermally driven valence tautomeric conversion in the solid state, and the pressure-induced transition takes place at a relatively low pressure ($P_c \sim 0.37$ GPa; see Table 2), being complete by 0.7 GPa. On the other hand, in the case of complex **B** that remains HS-Co^{II} down to 2.0 K, a much higher pressure is required to convert half of the HS-Co^{II} molecules to LS-Co^{III} molecules. The conversion is complete at the much higher pressure of 2.5 GPa. For both compounds the pressure induced transition is found to be completely reversible. Figure 8 shows that the results of increasing and decreasing pressure are nearly indentical. In these two compounds, the application of hydrostatic pressure does not produce crystal imperfections that modify the cooperativity of the phenomenon. Thus, application of pressure proves to be an effecient way of inducing the valence tautomeric interconversion.

(d) Mechanism of the Valence Tautomeric Transformation. There is one interesting question that remains about the mechanism of the valence tautomeric transformation: Does the transformation occur in one step (eq 3) or two steps (eq 4a,b)?

$$\text{HS-Co}^{II} \rightleftarrows \text{LS-Co}^{III} \qquad (3)$$

$$\text{HS-Co}^{II} \rightleftarrows \text{LS-Co}^{II} \qquad (4a)$$

$$\text{LS-Co}^{II} \rightleftarrows \text{LS-Co}^{III} \qquad (4b)$$

In the two-step mechanism the complex would first undergo a

(28) König, E.; Ritter, G.; Dengler, J.; Thuery, P.; Zarembowitch, J. *Inorg. Chem.* **1989**, *28*, 1757.
(29) (a) Gütlich, P. *Struct. Bonding (Berlin)* **1981**, *44*, 83. (b) König, E. *Prog. Inorg. Chem.* **1987**, *35*, 527. (c) Gütlich, P.; Hauser, A.; Spiering, H. *Angew. Chem., Int. Ed. Engl.* **1994**, *33*, 2024.

spin-crossover change at the cobalt ion upon decreasing the temperature. A further decrease in temperature would lead to an intramolecular electron transfer and a conversion from LS-Co^{II} to LS-Co^{III}. Obviously, in the one-step mechanism the spin-state change and the intramolecular electron transfer occur together. Preliminary data from three different quarters indicate that there may be more states of the system present than just the limiting HS-Co^{II} and LS-Co^{III} forms. Magnetic susceptibility data collected on a fine temperature grid for $[Co^{II}(3,5DTBSQ)_2(phen)]\cdot C_6H_5CH_3$ show that there is a very reproducible inflection occurring in a plot of n(HS-Co^{II}) vs temperature.[30] In agreement with this, heat capacity data collected for this same toluene solvate show a double-peaked heat capacity anomaly.[31] LCAO X_α calculations have also been carried out[32] for this complex (*sans tert*-butyl groups). These calculations indicate that, as far as the electronic energy is concerned, the three states of HS-Co^{II}, LS-Co^{II}, and LS-Co^{III} are relatively close in energy.

The present EXAFS data are in more accordance with the one-step mechanism but are not of high enough resolution to rule out definitively the two-step mechanism. Multiple-scattering calculations at the K-edge and X-ray absorption experiments at the cobalt $L_{II,III}$ edges, which are more sensitive than the K edge to the occupancy of the d orbitals, are planned to try to address the problem.

Acknowledgment. This work was supported by NSF Grant CHE-9420322 (D.N.H.) and NIH Grant HL-13652 (D.N.H.).

IC951080O

(30) Adams, D. M.; Hendrickson, D. N. Unpublished results.
(31) Adams, D. M.; Hendrickson, D. N.; Gütlich, P. Unpublished results.
(32) Adams, D. M.; Noodleman, L.; Hendrickson, D. N. Unpublished results.